J Solid State Electrochem (2013) 17:1449–1454
DOI 10.1007/s10008-013-2013-7

ORIGINAL PAPER

Electron transport in $CaMnO_{3-\delta}$ at elevated temperatures: a mobility analysis

Ekaterina I. Goldyreva · Ilya A. Leonidov · Mikhail V. Patrakeev · Victor L. Kozhevnikov

Received: 26 November 2012 / Revised: 21 January 2013 / Accepted: 22 January 2013 / Published online: 7 February 2013

Abstract The drift mobility of electron charge carriers in oxygen non-stoichiometric manganite $CaMnO_{3-\delta}$ was calculated by combining the total electrical conductivity and oxygen non-stoichiometry data at 700–950 °C and oxygen partial pressure varying between 10^{-6} and 1 atm. The carrier concentration changes with pressure and temperature were obtained with the help of the earlier-developed defect model involving reactions of oxygen exchange and thermal excitation of manganese sites. The activation energy for mobility is found to increase with oxygen non-stoichiometry. High-temperature electron transport properties of the manganite $CaMnO_{3-\delta}$ can be explained in terms of activated jumps of n-type small polarons in adiabatic regime. The relatively small mobility of charge carriers is explained by strong localization of polarons on manganese sites.

Keywords Calcium manganite · Perovskite · Electrical conductivity · Mobility of charge carriers · Small polarons

Introduction

Perovskite-like $CaMnO_{3-\delta}$ is an archetypal representative of manganites that have attracted considerable attention in recent years because of their interesting structural and electronic properties. Substitution of calcium for higher-charged cations and formation of vacancies in the oxygen sub-lattice both result in partial reduction of Mn^{4+} to Mn^{3+} cations and appearance of n-type conductivity [1–6]. The electron-doped derivatives $Ca_{1-x}R_xMnO_{3-\delta}$, where R is a rare earth metal, are stable in different atmospheres and exhibit rather large values of conductivity (σ) and negative thermopower (S) up to 1000 °C. These properties are of particular importance in thermoelectric devices for conversion of heat in electricity [7–13]. The substantially high electron conductivity, significant electrocatalytic activity, and moderate thermal expansion of $Ca_{1-x}R_xMnO_{3-\delta}$ make it possible to use these materials as cathodes of solid oxide fuel cells (SOFCs) and other electrochemical devices operating at elevated temperatures [14, 15]. In fact, their Sr-containing analogs are the state-of-the-art SOFC electrode compositions. Since the performance of thermoelectric and electrochemical devices is determined by the electron mobility and charge carrier concentration in manganites, the electron transport mechanisms in $CaMnO_{3-\delta}$ should be analyzed in the entire temperature range relevant for these applications.

According to [7, 12, 16], the high-temperature paramagnetic phases $Ca_{1-x}R_xMnO_{3-\delta}$ can be characterized as small polaron-type conductors where thermopower is described as [4, 17, 18]

$$S = -\frac{k_B}{e}\left(\ln\frac{N_n}{n} + \frac{E_S}{k_B T}\right) \quad (1)$$

Here, k_B is Boltzmann's constant, e is the absolute value of the electron charge, n is the concentration of polarons, N_n is number of available sites, and E_S is the energy difference between identical lattice distortions with and without the charge carrier. However, the increase of temperature from near 130 K to about 700 K is accompanied with the increase of absolute values of thermopower [7, 12, 16], which is in apparent disagreement with (1). The Hall mobility in paramagnetic $Ca_{1-x}La_xMnO_{3-\delta}$ is shown to increase with lanthanum content, i.e., with the concentration of charge carriers [19]. On the other hand, the increase in the amount

E. I. Goldyreva · I. A. Leonidov · M. V. Patrakeev · V. L. Kozhevnikov
Institute of Solid State Chemistry, Ural Branch, Russian Academy of Sciences, 620990, Ekaterinburg, Russian Federation

I. A. Leonidov (✉)
Ural Federal University, 620002, Ekaterinburg, Russian Federation
e-mail: leonidov@imp.uran.ru

of charge carriers in a small polaron conductor must be accompanied with the concomitant decrease in the amount of positions available for polaron jumps. Consequently, the trend for the mobility to decrease is expected, which is in controversy with the Hall data. Another unusual feature is a decrease of Hall mobility in $Ca_{1-x}La_xMnO_{3-\delta}$ ($0 \le x \le 0.1$) with the temperature increase at 130–300 K, which is particularly expressed in $CaMnO_{3-\delta}$. Based on these observations, authors [19] arrived at a conclusion about large polaron charge carriers in $CaMnO_{3-\delta}$ and its lightly electron-doped derivatives. The concentration of charge carriers in $CaMnO_{3-\delta}$ at room temperature does not exceed 0.001 per formula unit and is most possibly related with uncontrolled impurities [19]. It is reliably established that increase of δ in $CaMnO_{3-\delta}$ facilitates considerable increase of conductivity [1, 20].

Conductivity of n-type in $CaMnO_{3-\delta}$ with different stoichiometry is characterized with small values 0.02–0.16 eV of the activation energy E_σ at 150–600 K [1, 7, 13, 20–22]. Heating in air at 400–600 °C is accompanied with the increase of conductivity and with the increase of the activation energy E_σ to about 0.4 eV [7, 21]. At first glance, this behavior might be related to oxygen depletion at heating. However, any observable oxygen loss in $CaMnO_{3-\delta}$ occurs only at temperatures above 600 °C [23, 24]. Similarly, large E_σ values cannot be explained by phase transitions because low-temperature orthorhombic $CaMnO_{3-\delta}$ transforms to tetragonal phase only above 896 °C [25]. Thus, the mechanism of transport of charge carriers in $CaMnO_{3-\delta}$ at elevated temperatures seems to remain poorly understood at present.

On the whole, there have been quite a number of reports on electric properties of $CaMnO_{3-\delta}$ and related materials, but most of them dealt with properties at near room temperature or below. At the same time, studies in the high-temperature limit, where only most strong interactions survive, may help to better understand the nature of the state of $CaMnO_{3-\delta}$ that precedes the low-temperature states in electron-doped manganites. Moreover, some existing controversies on the nature of charge carriers in the manganites can be resolved when the data are obtained at most high temperatures possible. With this in mind, we focused the present study on conductivity and thermopower in $CaMnO_{3-\delta}$ at temperatures as high as 950 °C where the reaction of oxygen exchange with the ambient atmosphere is sufficiently intensive for obtaining equilibrium data, and oxygen deficiency may achieve large values before decomposition of the manganite occurs.

Experimental

The calcium manganite was obtained by firing metal organic precursors as described elsewhere [26]. The X-ray diffraction showed single-phase $CaMnO_{3-\delta}$ with the orthorhombic lattice parameters a=5.281(1), b=7.453(1), and c=5.266(1) Å. Rectangular bars 2×2×15 mm were cut from the sintered pellets for electrical measurements. One specimen, equipped with butt electrodes and thermocouples, was used for measurements of thermopower. The temperature gradient in the furnace along the sample was about 20 K/cm. Another specimen was used in four-probe measurements of the d.c. conductivity. Current leads of platinum wire (0.3 mm) were tightly wound to the sample at 14-mm spacing while the spacing between the potential probes was 10 mm. The specimen was placed perpendicular to another similar specimen for thermoelectric power measurements so that the temperature gradient along the sample at measurements of conductivity was zero. The measurements of conductivity and thermopower were carried out simultaneously in a cell utilizing oxygen sensing and pumping properties of cubically stabilized zirconia oxygen electrolyte as described elsewhere [27]. The electrical parameters were measured with a high-precision Solartron 7081 voltmeter. Experimental data points were collected only after equilibrium had been achieved between the sample and ambient oxygen gas, that is when changes in the logarithm of the conductivity did not exceed 0.01 %/min, and changes in thermopower did not exceed 0.001 μV/min. The measurements were carried out in isothermal runs at pressure decrease and halted upon achievement of the desirable low-pressure limit. Then, the oxygen pressure, p_{O_2}, was increased to the starting upper limit where measurements were repeated in order to confirm reversibility of the experiment; thereupon, temperature, T, was changed thus enabling the next measuring cycle.

Results and discussion

The variations of isothermal conductivity and thermopower with oxygen partial pressure p_{O_2} are shown in Fig. 1. The negative sign of thermopower suggests that n-type electron carriers are dominant in $CaMnO_{3-\delta}$ in the entire studied range of parameters T and p_{O_2}. The nonlinear shape of the plots in Fig. 1 is mostly related with rather sharp changes of oxygen non-stoichiometry δ at phase transitions that accompany changes in oxygen vacancy concentration in $CaMnO_{3-\delta}$ [26]. The combination of the earlier obtained variations of δ vs. p_{O_2} and T [26] with the data for σ and S can be used in order to find isothermal dependencies of conductivity and thermopower on oxygen content, Fig. 2. The thermopower plots in Fig. 2b suggest that the trend for the conductivity in Fig. 2a to increase with δ reflects, first of all, the respective increase in concentration of electrons, i.e., Mn^{3+} cations. Though less strong, the influence of temperature upon transport properties is quite viable also as can be seen from cross sections of the plots in Fig. 2 at constant

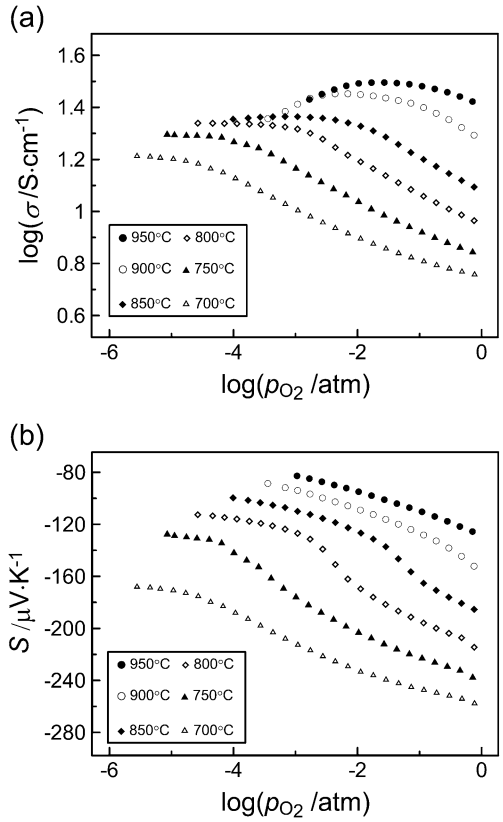

Fig. 1 Logarithmic isothermal plots of conductivity (**a**) and thermopower (**b**) depending on oxygen partial pressure

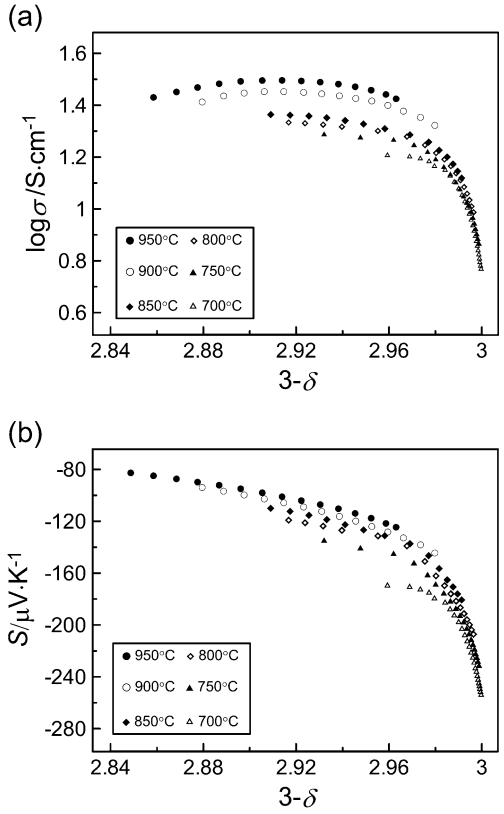

Fig. 2 Isothermal plots of conductivity (**a**) and thermopower (**b**) vs. oxygen content $(3-\delta)$ in $CaMnO_{3-\delta}$

values of $(3-\delta)$. The relevant plots in Arrhenius coordinates are presented in Fig. 3 where fields of existence are shown also for orthorhombic (O), tetragonal (T), and cubic (C) modifications of $CaMnO_{3-\delta}$ [26]. The slope of the log σT vs. $(1/T)$ plots corresponds to apparent activation energy for conductivity near 0.2 eV in orthorhombic and tetragonal phases while the conduction process in the cubic structure is characterized with a larger E_σ value equal approximately to 0.45 eV. The activation energy E_S for thermopower can be obtained from the slope of the plots in Fig. 3b. The respective values E_S are about 0.15 eV in both orthorhombic and cubic phases. It is seen from here that the inequality $E_S<E_\sigma$ characteristic for small polaron conductors [28] is always satisfied in the case of $CaMnO_{3-\delta}$.

It should be noticed that our values for E_σ in $CaMnO_{3-\delta}$ at δ=const exceed considerably the conductivity activation energy 0.01–0.08 eV in electron-doped manganites $Ca_{1-x}R_xMnO_3$ [7, 12, 16] where it virtually equals the mobility activation energy E_μ because the amount of charge carried is defined by the concentration of donors. The observed difference shows that heating can give rise to mobile n-type carriers in $CaMnO_{3-\delta}$ in addition to effects of non-stoichiometry. This conclusion is similarly corroborated by the activation energy $E_s\approx$0.15 eV, Fig.3b, much larger than the value of 0.01–0.04 eV in manganites $Ca_{1-x}R_xMnO_3$ where the concentration of carriers is fixed by the amount of impurities [18, 28].

Following Goodenough [29], the appearance of additional charge carriers at heating can be related to thermal excitation of electrons from the half-filled t_{2g} band to the empty e_g band of manganese cations

$$2Mn^{4+}(t_{2g}) = Mn^{3+}(e_g) + Mn^{5+}(t_{2g}) \quad (2)$$

This reaction may give a reasonable explanation to quite noticeable conductivity in $CaMnO_{3-\delta}$ at $\delta\rightarrow 0$, Fig. 2a. Before discussing mobility and conduction mechanism, we need in the first place to understand how concentration of electrons, i.e., of Mn^{3+} cations, changes with temperature. It can be shown [30] that concentrations n, g, and p of differently charged manganese species Mn^{3+}, Mn^{4+}, and Mn^{5+}, respectively, and oxygen non-stoichiometry are interrelated as

$$n = 2\delta + \frac{\delta + 2K - 4\delta K - D}{4K - 1} \quad (3)$$

$$g = 1 - 2\delta - \frac{2(\delta + 2K - 4\delta K - D)}{4K - 1} \quad (4)$$

Here, $K=n\times p/g^2$ is the equilibrium constant for reaction (2) and $D = \sqrt{K - 4\delta^2 K + \delta^2}$. It follows from (3) and (4)

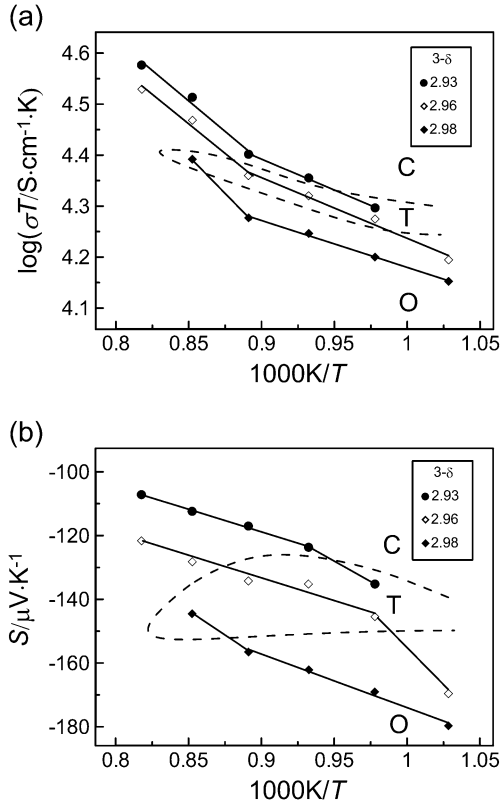

Fig. 3 Arrhenius plots for conductivity (**a**) and thermopower (**b**) at permanent values of oxygen content ($3-\delta$) in $CaMnO_{3-\delta}$. The existence fields [26] for orthorhombic (*O*), tetragonal (*T*), and cubic (*C*) structural modifications are shown with *dashed lines*

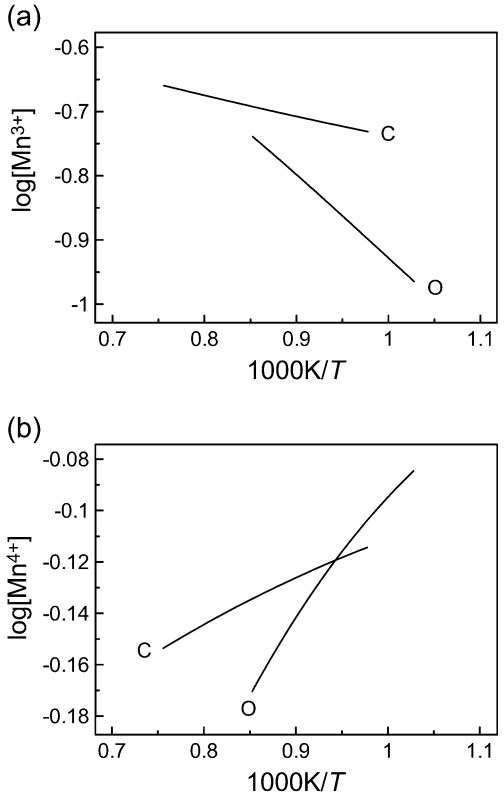

Fig. 4 Arrhenius plots for concentration of Mn^{3+} (**a**) and Mn^{4+} (**b**) cations in orthorhombic (δ=0.02) and cubic (δ=0.07) structural modifications of $CaMnO_{3-\delta}$

that at invariable oxygen non-stoichiometry, the changes in concentrations *n*, *g*, and *p* are governed by temperature dependence of the equilibrium constant

$$K = \exp(\Delta S^{\circ}/R)\exp(-\Delta H^{\circ}/RT), \quad (5)$$

where ΔS° and ΔH° designate entropy and enthalpy, respectively, for reaction (2). The temperature variations of parameters *n* and *g* can be calculated from (3) and (4) with the use of ΔS° and ΔH° obtained elsewhere [30]. The results for δ=0.02 and 0.07 are shown in Fig. 4. As expected, the concentration of Mn^{3+} cations noticeably increases with temperature due to reaction (2). For instance, the straightforward contribution of non-stoichiometry in the right hand side of Eq. (3) at 900 °C is 2δ=0.04 while the overall value for *n* achieves about 0.18. More considerable increase of *n* with temperature in the orthorhombic than in the cubic phase reflects respectively larger enthalpy ΔH° for reaction (2) in the orthorhombic structure. Notice additionally that thermodynamic equilibrium data result in ΔH° values equal 0.8 and 0.35 eV in orthorhombic and cubic polymorphs of $CaMnO_{3-\delta}$, respectively [30], which coincide fairly well with the calculated band gap values 0.7 and 0.46 eV [31]. Considering the known relation $E_{\sigma}=\Delta H^{\circ}/2+E_{\mu}$ and neglecting the relatively small contribution of the mobility activation energy, we arrive at the estimation $E_{\sigma}\approx$ 0.4 eV that is in a good match with the activation energy for conductivity in orthorhombic $CaMnO_{3-\delta}$ at 400–600 °C [7, 21].

The obtained concentration of n-type carriers enables immediate calculation of their mobility as

$$\mu = \frac{\sigma}{e \cdot n \cdot N}, \quad (6)$$

where the number *N* of formula units per 1 cm^3 can be derived from structural data [32, 33]. The resulting mobility values vary within 0.03–0.05 $cm^2V^{-1}s^{-1}$ as can be seen in Fig. 5 where data for orthorhombic and cubic phases are

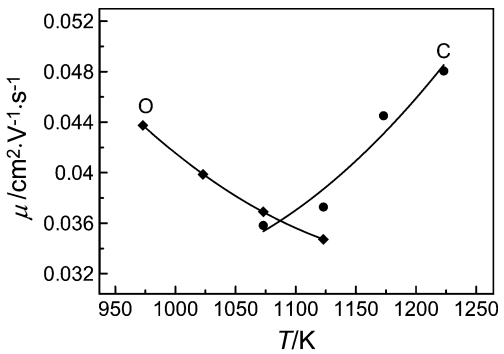

Fig. 5 Mobility vs. temperature plot in orthorhombic (δ=0.02) and cubic (δ=0.07) structural modifications of $CaMnO_{3-\delta}$

shown. The data for the intermediate, tetragonal phase are less representative because of the relatively narrow field of existence; therefore, the tetragonal phase is omitted from further consideration. The estimates of mobility do not involve any assumptions concerning conduction mechanism and seem rather robust. Hence, the mobility appreciably smaller than the characteristic value 0.1 $cm^2V^{-1}s^{-1}$, which is considered as a threshold separating small polaron and band conductors [17], gives a strong evidence to high-temperature conductivity in $CaMnO_{3-\delta}$ mediated by small polaron charge carriers.

One can notice that temperature dependences of electron mobility have different trends in orthorhombic and cubic structural modifications. The mobility values increase with temperature in the cubic phase as is expected in a small polaron conductor. At the same time, the temperature dependence of mobility in the orthorhombic phase is in apparent disagreement with the small polaron conduction mechanism. In order to understand this behavior, we need to consider expression [34] for mobility of small polarons

$$\mu = \frac{er^2 g\nu}{k_B T} \exp\left(-\frac{E_\mu}{k_B T}\right) \quad (7)$$

where r is the jump length; the jump frequency ν is approximately equal to the frequency of optical phonons ν_0 in the adiabatic limit, while the condition $\nu << \nu_0$ is satisfied in the case of nonadiabatic polarons. It is seen from (7) that when the activation energy is small enough, the respectively weak exponential increase of mobility with temperature may occur overwhelmed by the temperature-driven decrease of the preexponential multiplier. The decrease in the amount of transfer sites, g, can occur additionally at temperature increase as is seen in Fig.4b for orthorhombic $CaMnO_{3-\delta}$. Therefore, the correct evaluation of the mobility activation energy E_μ ought to be done from the plots $\log(\mu T/g)$ vs. $1/T$ at constant δ values as shown for δ=0.02 and δ=0.07 in Fig. 6. Considering uncertainties that can achieve 10–15 % in the calculated concentration of electrons at 700–750 °C, Fig.4a, the evaluation of the activation energy in the orthorhombic phase gives E_μ=0.05–0.10 eV. This value is comparable with the average heat energy kT. It is for this reason that mobility may have a metal-like behavior in Arrhenius plots. This situation is not unique, and it was observed earlier in lightly doped manganites $Ca_{1-x}La_xMnO_{3-\delta}$ where the concentration of n-type carriers is fixed by the amount of donor impurities [7, 12]. Similar estimation of the mobility activation energy in the cubic phase at δ=0.07 gives E_μ=0.35–0.40 eV.

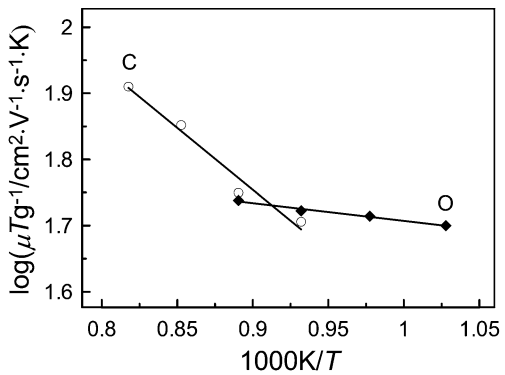

Fig. 6 Arrhenius plot for mobility in orthorhombic (δ=0.02) and cubic (δ=0.07) structural modifications of $CaMnO_{3-\delta}$

The obtained values for the mobility activation energy can be used further in order to estimate the jump frequency of polarons from Eq. (7). The concentration g of Mn^{4+} cations can be taken from Fig.4b. The jump length can be approximated by the distance between neighboring manganese cations, i.e., by the reduced parameter of the perovskite pseudo cell a≈3.73 Å. In the result, the calculated jump frequency that occurs equals $5.5\cdot10^{12}$ and $1.5\cdot10^{14}$Hz in orthorhombic and cubic phase, respectively, which is in a good correspondence with the frequency range 10^{13}–10^{14} Hz of optical phonons in similar perovskites [18, 35].

The estimates for mobility and jump frequency obtained from measurements at high temperatures between 700 and 950 °C as well as at more moderate heating at 20–700 °C [7, 12] consistently support adiabatic n-type small polaron transport in $CaMnO_{3-\delta}$. Small mobility values give evidence to rather strong localization of electrons on manganese cations. In contrast with other non-stoichiometric perovskites with a wide forbidden gap, e.g., ferrites, where the concentration of charge carriers depends mostly on deviation δ from stoichiometry [36, 37], calcium manganite $CaMnO_{3-\delta}$ is distinguished by a considerable difference in the activation energy for conductivity and mobility. This feature is related with the band gap, which is small enough in both orthorhombic and cubic phases, so that a rather large amount of thermally excited electrons may appear at heating and take part in the conduction process at elevated temperatures.

Acknowledgments The authors gratefully acknowledge partial support of this work by the Russian Foundation for Basic Research (grant nos. 10-03-00475a and 12-03-31217) and the Presidium of Ural Branch of RAS (grant nos. 12-M-23-2061).

References

1. Zeng Z, Greenblatt M, Croft M (1999) Phys Rev B 59:8784–8788
2. Chiorescu C, Neumeier JJ, Cohn JL (2006) Phys Rev B 73:014406
3. Martin C, Maignan A, Damay F, Hervieu M, Raveau B (1997) J Solid State Chem 134:198–202
4. Hejtmánek J, Jirák Z, Maryško M, Martin C, Maignan A, Harvieu M, Raveau B (1999) Phys Rev B 60:14057–14065
5. Sudheendra L, Raju AR, Rao CNR (2003) J Phys Condens Matter 15:895–905
6. Caspi EN, Avdeev M, Short S, Jorgensen JD, Lobanov MV, Zeng Z, Greenblatt M, Thiyagarajan P, Botez CE, Stephens PW (2004) Phys Rev B 69:104402

7. Ohtaki M, Koga H, Tokunaga T, Eguchi K, Arai H (1995) J Solid State Chem 105:105–111
8. Matsubara I, Funahashi R, Takeuchi T, Sodeoka S, Shimisu T, Ueno K (2001) Appl Phys Lett 78:3627–3629
9. Thao PX, Tsuji T, Hashida M, Yamamura Y (2003) J Ceram Soc Jap 111:544–547
10. Reddy ES, Noudem JG, Hebert S, Goupil C (2003) J Phys D: Appl Phys 38:3751–3755
11. Flahaut D, Mihara T, Funahashi R, Nabesima N, Lee K, Ohta H, Koumoto K (2001) J Appl Phys 100:084911
12. Wang Y, Sui Y, Wang X, Su W (2009) J Phys D: Appl Phys 42:055010
13. Ohtaki M (2011) J Ceram Soc Jap 119:770–775
14. Adler SB (2004) Chem Rev 104:4791
15. Tsipis EV, Kharton VV (2008) J Solid State Electrochem 12:1367–1391
16. Maignan A, Martin C, Damay F, Raveau B, Hejtmánek J (1998) Phys Rev B 58:2758–2763
17. Bosman IG, Daal HJ (1970) Adv Phys 19:1–117
18. Jaime M, Salamon MB, Rubinstein M, Treece RE, Horwitz JS, Chrisey DB (1996) Phys Rev B 54:11914–11917
19. Cohn JL, Chiorescu C, Neumeier JJ (2005) Phys Rev B 72:024422
20. Taguchi H (1985) Phys Stat Sol (a) 88:K79–K82
21. Melo Jorge ME, Nunes MR, Silva Maria R, Sousa D (2005) Chem Mater 17:2069–2075
22. Souza JA, Neumeier JJ, Bollinger RK, McGuir B, Santos CAM, Terashita H (2007) Phys Rev B 76:024407
23. Rørmark L, Wiik K, Stølen S, Grande T (2002) J Mater Chem 12:1058–1067
24. Dabrowski B, Chimaissem O, Mais J, Kolesnik S, Jorgensen JD, Short S (2003) J Solid State Chem 170:154–164
25. Taguchi H, Nagao M, Sato T, Shimada M (1989) J Solid State Chem 78:312–315
26. Leonidova EI, Leonidov IA, Patrakeev MV, Kozhevnikov VL (2011) J Solid State Electrochem 15:1071–1075
27. Patrakeev MV, Mitberg EB, Lakhtin AA, Leonidov IA, Kozhevnikov VL, Kharton VV, Avdeev M, Marques FMB (2002) J Solid State Chem 167:203–213
28. Hundley MF, Neumeier JJ (1997) Phys Rev B 55:11511–11515
29. Goodenough JB (1966) J Appl Phys 37:1415–1422
30. Goldyreva EI, Leonidov IA, Patrakeev MV, Kozhevnikov VL (2012) J Solid State Electrochem 16:1187–1191
31. Søndenå R, Stølen S, Ravindran P, Grande T, Grande NL (2007) Phys Rev B 75:184105
32. Poeppelmeier KR, Leonowicz ME, Scanlon JC, Longo JM, Yelon WB (1982) J Solid State Chem 45:71–79
33. Chmaissem O, Dabrowski B, Kolesnik S, Mais J, Brown DE, Kruk R, Prior P, Pyles B, Jorgensen JD (2001) Phys Rev B 64:134412
34. Mott N (1987) Conduction in non-crystalline materials. Clarendon, Oxford
35. Karim DP, Aldred AT (1979) Phys Rev B 20:2255–2260
36. Mogni L, Fouletier J, Prado F, Caniero A (2005) J Solid State Chem 178:2715–2723
37. Markov AA, Patrakeev MV, Savinskaya OA, Nemudry AP, Leonidov IA, Leonidova ON, Kozhevnikov VL (2008) Solid State Ionics 179:99–103